Science of the Total Environment 765 (2021) 142681

Contents lists available at ScienceDirect

Science of the Total Environment

journal homepage: www.elsevier.com/locate/scitotenv

Radiofrequency at 2.45 GHz increases toxicity, pro-inflammatory and pre-apoptotic activity caused by black carbon in the RAW 264.7 macrophage cell line

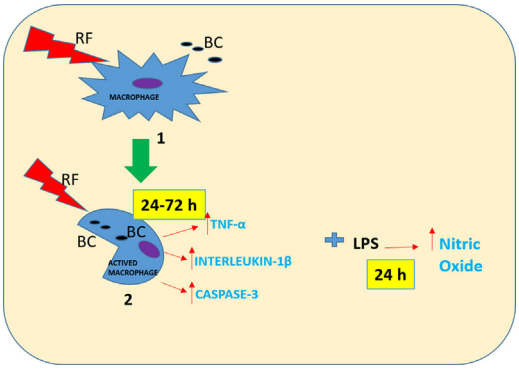
Rosa Ana Sueiro-Benavides [a], Jose Manuel Leiro-Vidal [a], Aarón Ángel Salas-Sánchez [b,c], J. Antonio Rodríguez-González [b], Francisco J. Ares-Pena [b], M. Elena López-Martín [d,*]

[a] Research Institute on Chemical and Biological Analysis, Dept. of Microbiology and Parasitology, University of Santiago de Compostela, E-15782 Santiago de Compostela, Spain
[b] CRETUS Institute, Dept. Applied Physics, Faculty of Physics, University of Santiago de Compostela, E-15782 Santiago de Compostela, Spain
[c] ELEDIA@UniTN – DISI – University of Trento, 38123, Trentino-Alto Adige, Italy
[d] CRETUS Institute, Dept. Morphological Sciences, Faculty of Medicine, University of Santiago de Compostela, E-15782 Santiago de Compostela, Spain

HIGHLIGHTS

- Black carbon and radiofrequency could be a suitable model for accelerated cellular toxicity.
- Electromagnetic fields and fine/coarse black carbon prolong innate and inflammatory immune responses.
- 2.45 GHz radiofrequency and black carbon activate apoptosis of the RAW 264.7 macrophage cell line.

GRAPHICAL ABSTRACT



ARTICLE INFO

Article history:
Received 26 July 2020
Received in revised form 15 September 2020
Accepted 20 September 2020
Available online 4 October 2020

Editor: Daqiang Yin

Keywords:
RAW 264.7 cells
Black carbon, electromagnetic fields
Gigahertz transverse electromagnetic cell
Specific absorption rate
Tumor necrosis factor-alpha
Interleukin-1β
Caspase-3

ABSTRACT

Environmental factors such as air pollution by particles and/or electromagnetic fields (EMFs) are studied as harmful agents for human health. We analyzed whether the combined action of EMF with fine and coarse black carbon (BC) particles induced cell damage and inflammatory response in RAW 264.7 cell line macrophages exposed to 2.45 GHz in a gigahertz transverse electromagnetic (GTEM) chamber at sub-thermal specific absorption rate (SAR) levels. Radiofrequency (RF) dramatically increased BC-induced toxicity at high doses in the first 24 h and toxicity levels remained high 72 h later for all doses. The increase in macrophage phagocytosis induced after 24 h of RF and the high nitrite levels obtained by stimulation with lipopolysaccharide (LPS) endotoxin 24 and 72 h after radiation exposure suggests a prolongation of the innate and inflammatory immune response. The increase of proinflammatory cytokines tumor necrosis factor-α, after 24 h, and of interleukin-1β and caspase-3, after 72 h, indicated activation of the pro-inflammatory response and the apoptosis pathways through the combined effect of radiation and BC. Our results indicate that the interaction of BC and RF modifies macrophage immune response, activates apoptosis, and accelerates cell toxicity, by which it can activate the induction of hypersensitivity reactions and autoimmune disorders.

© 2020 Elsevier B.V. All rights reserved.

* Corresponding author at: Departamento de Ciencias Morfológicas, Facultad de Medicina, Universidade de Santiago de Compostela, C/ San Francisco s/n, 15782 Santiago de Compostela, Spain.
E-mail addresses: rosaana.sueiro@usc.es (R.A. Sueiro-Benavides), josemanuel.leiro@usc.es (J.M. Leiro-Vidal), aaronangel.salas@usc.es (A.Á. Salas-Sánchez), ja.rodriguez@usc.es (J.A. Rodríguez-González), francisco.ares@usc.es (F.J. Ares-Pena), melena.lopez.martin@usc.es (M.E. López-Martín).

https://doi.org/10.1016/j.scitotenv.2020.142681
0048-9697/© 2020 Elsevier B.V. All rights reserved.

1. Introduction

Genetic and environmental factors work together in the emergence and development of many diseases in modern society (Adams et al., 2010). Among the environmental factors, air pollution from particulate matter (PM) and other harmful substances are strongly associated with inflammatory and autoimmune diseases (Anaya, 2012). The immediate, local impact of inhaled particles is very obvious, but it is difficult to know how PM can affect, initiate or aggravate autoimmune processes (Ritz, 2010; Gawda et al., 2018). Environmental soot from black carbon (BC) in a size range of 10 nm–1 mm (Wang et al., 2014) is the largest component of PM and causes premature human mortality and disability (Goto, 2014). BC can provoke a chronic inflammatory condition and plays a fundamental role in the development of cancer, cardiovascular dysfunction and respiratory diseases (Niranjan and Thakur, 2017). It causes direct toxicity and produces oxidative stress by affecting the mitochondria and initiating apoptosis, autophagy (Jing et al., 2019) and increased calcium intake (Deweirdt et al., 2020). BC also provokes systemic toxicity by causing secretion of inflammatory mediators and cytokines, which amplify the immune response (Patel et al., 2013). The presence of this very damaging air component in European countries has motivated research to discover efficient, economic ways to measure and monitor PM pollution (Salas-Sánchez et al., 2020).

The widespread use of new wireless technologies and applications has created a need for studies on the health effects of electromagnetic fields (EMFs). There is strong evidence that long-term exposure to certain EMF sources constitute a risk factor for certain types of cancer (Belyaev et al., 2016). Similarly, numerous studies on the effects of Wi-Fi in the 2.45 GHz bandwidth have shown it to cause oxidative stress, apoptosis, cellular DNA damage and calcium overload (Pall, 2018). In prior research on continuous and combined exposure to two radiofrequencies (RF) of 2.45 and 0.9 GHz, we also found decreased phagocytic activity, increased inflammation and cytoprotective or cytotoxic responses along with evidence of cellular stress and increased pre-apoptotic activity (López-Furelos et al., 2018, 2016).

Human life and reality involve exposure to combined stressors (Kostoff et al., 2018). Numerous studies have shown that stress factors, chemical cytotoxins and physical factors can influence normal cellular function (Wójcik-Piotrowicz et al., 2017). Our general ignorance about the biological effects of electromagnetic fields in dependence on the action of other agents has makes it necessary to develop laboratory models to test hypotheses about the combined and/or simultaneous effects of exposure of environmental particles and non-ionizing electromagnetic radiation, as we have already suggested (Salas-Sánchez et al., 2019). The possibilities of additive effects, antagonism, synergy or facilitation between electromagnetic fields and pollution agents should be investigated (Kostoff and Lau, 2013). Macrophages play an essential role in orchestrating the inflammatory responses induced by exposure to air pollutants and in interaction with electromagnetic fields, as evidenced in the use of macrophage cell lines to test for environmental pollutants (Hiraiwa and Van Eeden, 2013; Jalava et al., 2009; López-Furelos et al., 2018). To discover how combined exposure to BC particles and electromagnetic fields affects the innate immune response and cell viability, RAW 264.7 cell line macrophages (RAW) were exposed to 2.45 GHz RF for 24 or 72 h in a gigahertz transverse electromagnetic test chamber (GTEM). Several innate immune functions were then studied and evaluated, including: oxidative stress through the quantification of nitric oxide (NO) production after stimulation with bacterial lipopolysaccharide (LPS), phagocytic activity, proinflammatory activity by determining cytokine expression of tumor necrosis factor-alpha (TNF-α) and interleukin-1β (IL-1β), and pre-apoptotic activity measured through caspase-3 gene expression.

2. Material and methods

2.1. Cell culture

The experiments were conducted with the RAW murine macrophage cell line, acquired from the American Type Culture Collection (ATCC®, USA), which is routinely cultured in Iscove's Modified Dulbecco's Medium (IMDM; GibcoTM, Paisley, UK), supplemented with 3.024 mg/l $NaHCO_3$ and 10% of heat-inactivated foetal bovine serum (FBS; GibcoTM). Cells were maintained sub-confluent at 37 °C in humidified air containing 5% CO_2.

Three different culture media were used: 1) In the sub-confluent cultures (70–90%) of the RAW cells, 90% of the old IMDM medium was removed. The cells were mechanically re-suspended by scraping (plastic scraper), then transferred to a new 75 cm^2 flask (Thermo Fisher Scientific, Waltham, MA, USA) at 1:3 to 1:6 concentration, depending on the initial cell concentration obtained (from a culture flask to 3 or 6), and new medium was added. The flasks were incubated horizontally under conditions of 5% CO_2 at 37 °C. The new medium had to be tempered at 37 °C before using it for renewal. 2) Leibovitz L-15 medium (GibcoTM) was used during radiation to avoid the use of a CO_2 incubator, as its formula does not contain bicarbonate as a buffer. L-15 medium also requires growth factors, so 10% FBS was added. 3) Dulbecco's Modified Eagle Medium/F-12 Nutrient Mixture 1:1 containing 2 mM L-glucosamine and 15 mM HEPES (DMEM, GibcoTM) and supplemented with 10% FBS was used to perform the NO and MTT assays, to avoid interferences in the results associated with the phenol red pH indicator that was present in the other media used in the study.

2.2. Characteristics of particulate samples

Glassy spherical BC powder measuring 0.4–12 μm (Thermo Fisher Scientific MFCD00133992 Kandel, Germany) was used in this study. The compound was prepared as 1 g/ml stock solutions in dimethyl sulphoxide (DMSO) and kept in the dark at room temperature until use. The stocks were diluted just prior to use in IMDM, DMEM or L-15 medium containing 10% FBS to obtain the final concentrations required for each assay.

2.3. Experimental design

The experimental groups (G) were divided according to the following experimental design:

- G1: Non-irradiated control cell cultures studied after 24 h.
- G2: Cell cultures with 1.5 μg/ml (G2A) or 150 μg/ml (G2B) BC without irradiation and studied after 24 h.
- G3: Cell cultures irradiated for 24 h.
- G4: Cell cultures with 1.5 μg/ml (G4A) or 150 μg/ml (G4B) BC and irradiated for 24 h.
- G5: Non-irradiated control cultures studied after 72 h.
- G6: Cell cultures with 1.5 μg/ml (G6A) or 150 μg/ml (G6B) BC without irradiation and studied after 72 h.
- G7: Cell cultures irradiated for 72 h.
- G8: Cell cultures with 1.5 μg/ml (G8A) or 150 μg/ml (G8B) BC and irradiated for 72 h.

See Table 1.

2.4. Experimental radiation system

In this work, an experimental radiation system analogous to the one described in López-Furelos et al. (2018) was used, except that only one frequency was applied (2.45 GHz) instead of the two (0.9 and 2.45 GHz) analyzed in that work (López-Furelos et al., 2018). The exposure setup involved amplifying a 2.45 GHz pure sinusoidal signal from a vector

Table 1
Experimental design groups.

Groups	Treatment
G1	RAW non-RAD 24 h
G2A	RAW BC 1.5 μg/ml + no RAD 24 h
G2B	RAW BC 150 μg/ml + no RAD 24 h
G3	RAW RAD 24 h
G4A	RAW BC 1.5 μg/ml + RAD 24 h
G4B	RAW BC 150 μg/ml + RAD 24 h
G5	RAW non-RAD 72 h
G6A	RAW BC 1.5 μg/ml + no RAD 72 h
G6B	RAW BC 150 μg/ml + no RAD 72 h
G7	RAW RAD 72 h
G8A	RAW BC 1.5 μg/ml + RAD 72 h
G8B	RAW BC 150 μg/ml + RAD 72 h

signal analyzer and transmitting it to a GTEM chamber. An isotropic probe was used to measure the field and determine the peak value. This measurement was taken before placing the culture flask cells in the chamber and adjusting a desired transmitted power of the signal. Since it is possible to define the behavior of the chamber in the measurement zone, these resulting values were used to create a simulation of the GTEM chamber using three flat wave fronts that reproduced the data obtained with the probe.

The electromagnetic parameters used in this experimental radiation system and the simulation results related to the calculated finite-difference time-domain (FDTD) are the SAR of these cell cultures. The SAR represents a quantity of energy absorbed by the tissue and it is described in Table 2. SAR values were estimated using SEMCAD X (FDTD)-based software (Schmid and Partner Engineering, 2009). An automatic thermoregulation system was designed to maintain a constant temperature of 37 °C, as described by López-Furelos et al. (2018).

2.5. Radiation protocol

RAW cells were inoculated into 25 cm^2 culture flasks (Thermo Fisher Scientific, Waltham, MA, USA) containing 20 ml of L15 medium supplemented with 10% FBS (at final concentration of 1×10^6 cells/ml). The IMDM culture medium was replaced with L-15 medium during this experimental phase of the study. Then, the cells were exposed to radiation for 24 or 72 h in the GTEM chamber (two cell cultures per group and time) at the point of maximum field uniformity, with the culture flask placed horizontally and the flask cup oriented towards the source of radiation.

The non-irradiated experimental groups were simultaneously incubated in L15 medium supplemented with 10% FBS for 24 or 72 h at 37 °C.

2.6. Cell viability analysis

2.6.1. MTT assay

Initially, the MTT (4,5-dimethyl-2-thiazolyl-2,5-diphenyl tetrazolium) method was used. When this light-yellow substance is reduced by living cells, it produces formazan, which is dark blue. This process requires active mitochondria, so when cells die, formazan production decreases significantly. Cells (at a density of 1×10^5/well) were incubated for 24 h at 37 °C with 5% CO2 in 96-well plates containing medium without phenol red (DMEM) and 10% FBS in a final volume of 100 μl. Then, the cells were incubated at 37 °C with 50 μl/well of MTT solution (1 mg/ml in PBS) for 4 h. Subsequently, the plate was centrifuged at 700*g* for 10 min, the medium was removed by aspiration and the cells were solubilized in DMSO (100 μl) for 10 min. Finally, optical density was measured at 540 nm using a microplate reader (Kumar et al., 2018). The cell viability was calculated according to the following formula: (%) = (OD of RAW + BC − OD of BC) / (OD of RAW − OD of DMEM only) × 100 (Supplementary material).

Table 2
Experimental conditions of the experimental groups subjected to RF radiation.

				Mean SAR (W/kg)
f (MHz)	P_{TR} (W)	E_m (V/m)	P_D (W/m^2)	Culture flasks
2450	12	102.8	28.0	0.4060

f: frequency; P_{TR}: transmitted power, E_m: measured r.m.s. electrical field strength, P_D: incident power density; mean SAR: FDTD-calculated specific absorption rate using E_m.

2.6.2. Trypan Blue assay

RAW cell viability was also measured by staining with Trypan Blue vital dye (Sigma-Aldrich St. Louis, MO, USA). After 24 or 72 h of treatment, aliquots of 1×10^5 cells from each experimental group were collected in a screw-cap test tube and centrifuged at 450 ×*g* for 5 min. The cell pellet was re-suspended in 500 μl of L15 medium without serum and then 100 μl of 0.4% trypan blue stain in sterile phosphate buffered saline (PBS; pH 7.2) was added to each cell suspension. The mixture was incubated for 5 min at room temperature. Viable cells were counted using a Neubauer haemocytometer under a light microscope (Nikon Eclipse E-600, Japan). Trypan blue is reactive because the chromophore is negatively charged and does not interact with the cell unless the membrane is damaged. Therefore, all cells that exclude the dye are viable. The cell suspension was inoculated in the haemocytometer, then 4 upper quadrants and 4 lower quadrants measuring 1x1mm each were counted. Total live cells (without trypan blue staining) and dead cells (with trypan blue staining) were counted and a percentage was obtained for each group in relation to the total number of cells in all the 4 upper and lower quadrants. The viability of each group was measured with the trypan blue cell test, using 6 samples per group.

2.7. Phagocytic activity

Phagocytic activity was determined from aliquots collected in culture flasks containing RAW cells in L15 medium with 10% FBS and treated with BC (final BC concentration of 150 and 1.5 μg/ml) for 24 or 72 h and in culture flasks subjected to combined radiation and BC treatment at both previously indicated concentrations and treatment times. The phagocytic activity of macrophages was evaluated on slides containing 10 μl of cells per sample, previously fixed with 10% neutral buffered formalin (10% formalin in PBS, pH 7,2). Phagocytic activity was evaluated by 100× light microscopy (Nikon Eclipse E600) with immersion oil in 100 cells (groups G2, G6 and groups G4, G8). Each macrophage was examined to determine whether it had phagocytosed or not, and the BC particles were evaluated in 25 of the 100 macrophages per group. Semi-quantitative measurement of the number of particles that were adhered to or internalized within the macrophage was also recorded (0–5; 5–10 and more than 10) (see Tables 3A and 3B). An overall calculation of the macrophages that had phagocytosed or with adhered particles was established to determine the average phagocytic capacity of each group, establishing a percentage for each set of 25 macrophages out of the 100 measured per group.

Table 3A
Semi-quantitative determination of individual radiated cells at 24 h.

RAW BC 1.5 μg/ml + RAD 24 h	RAW BC 1.5 μg/ml + no RAD 24 h	RAW BC 150 μg/ml + RAD 24 h	RAW BC 150 μg/ml + no RAD 24 h
50: 0	64:0	1:0	9:0
38:+	31:+	24:+	42:+
10:++	5:++	32:++	19:++
2:+++	0:+++	43:+++	30:+++

Means 0 = No phagocytosis; + = 0–5 phagocytosed particles; ++ = 5–10 phagocytosed particles; +++ = more than 10 phagocytosed particles.

Table 3B
Semi-quantitative determination of individual radiated cells at 72 h.

RAW BC 1.5 μg/ml + RAD 72 h	RAW BC 1.5 μg/ml + no RAD 72 h	RAW BC 150 μg/ml + RAD 72 h	RAW BC 150 μg/ml + no RAD 72 h
11: 0	19:0	8:0	10:0
49:+	46:+	19:+	50:+
30:++	30:++	32:++	21:++
10:+++	5:+++	41:+++	19:+++

Means 0 = No phagocytosis; + = 0–5 phagocytosed particles; ++ = 5–10 phagocytosed particles; +++ = more than 10 phagocytosed particles.

2.8. Assay of nitrite production (NO assay)

After 24 or 72 h of radiation exposure (groups G2, G3, G4 and G7), all RAW cells (Groups G1–G8) were centrifuged 450 ×*g* for 5 min. The L-15 culture medium was removed and the pellets were re-suspended in DMEM with 10% FBS. Then, 100 μl aliquots (1×10^6 cells/ml) were stimulated with LPS and incubated in microplates (Thermo Fisher Scientific, Waltham, MA, USA) for 24 or 72 h at 37 °C with 5% CO_2 to perform the NO assay. LPS was prepared as 1 mg/ml stock solution in PBS and stored in the dark at −20 °C until use. The resulting stock was diluted in DMEM medium and adjusted to the final concentration of 100 ng/ml (10 ng/well) just before use. NO production was estimated on the basis of nitrite production in macrophage culture supernatants, measured by the Griess reaction. One-hundred microliter were removed from each well and incubated with an equal volume of Griess reagent: 1% sulfanilamide (Merck, Kenilworth, NJ, USA) and 0.1% naphthylethylenediamine hydrochloride (Merck,) in 2.5% phosphoric acid (Sigma, St. Louis, MO, USA). The reaction required incubation for 10 min at room temperature (Leiro et al., 2004). NO production was estimated after incubation (24 or 72 h) and the results were measured at 530 nm in an ELISA reader (ELx808, Biotek, Winooski, VT, USA). Nitrite concentration was calculated against a standard curve obtained from $NaNO_2$ (1–200 μM) in culture medium. The results were compared with their respective controls.

2.9. Detecting gene expression

2.9.1. mRNA extraction

After each treatment, the RAW cells were centrifuged at 450 ×*g* for 5 min. The L-15 culture medium was removed and the pellets resuspended in 1 ml of TriPure reagent (Sigma-Aldrich, St. Louis, MO, USA). Then, 0.2 ml of chloroform (Merck, Kenilworth, NJ, USA) was added and the culture was incubated for 10 min before centrifuging at 12000 ×*g* and 4 °C for 15 min. The phase containing the DNA, proteins and cell debris was discarded and the supernatant fraction containing the RNA was kept. To remove the TriPure reagent residues, the cultures were rinsed with isopropyl alcohol (Merck) followed by 70% ethanol (Merck), and centrifuged after each wash. The dehydrated pellet was stored at −80 °C.

2.9.2. DNAse treatment

The pellet was hydrated in H_2O with diethylpyrocarbonate (Sigma-Aldrich, St. Louis, MO) and incubated for 15 min at 60 °C. Subsequently, the RNA was quantified using NanoDrop ND-1000 equipment (Thermo Fisher Scientific, Waltham, MA, USA). For DNase treatment, a commercial kit (Thermo Fisher Scientific, Waltham, MA, USA) consisting of DNase I and a reaction buffer with 2.5 mM $MgCl_2$ was used. After incubation for 30 min at 37 °C, the reaction was stopped with 50 mM EDTA from the kit.

2.9.3. RT-qPCR

We combined 200 ng of the pure RNA sample with 1.25 μM random hexamer primers (Roche, Basel, Switzerland) and 250 μM deoxynucleoside triphosphate (dNTPs) then allowed it to incubate at 65 °C for 5 min. Reagents were then added from the GeneAmp® RNA PCR kit (Thermo Fisher Scientific, Waltham, MA, USA), consisting of 200 U of MMLV (Moloney murine leukemia virus) reverse transcriptase (Promega, Madison, WI) in a reaction buffer of 30 mM Tris and 20 mM KCl (pH 8.3) and ribonuclease inhibitor. These were then introduced into a thermocycler (T100™ Thermal Cycler, Bio-Rad, Watford, UK) that was programmed as follows: 25 °C for 5 min, 37 °C for 50 min and 70 °C for 15 min. As a result, we obtained the cDNA of the total mRNA.

Once the cDNA had been synthesized, we performed a real-time quantitative PCR (qPCR) analysis to study TNF-α, IL-1β and caspase-3 gene expressions. The β-actin (ACT) primer pair was used to normalize the data, which were expressed in relative arbitrary units (primers used are shown in Table 4). Each sample was introduced in triplicate onto a multi-well plate (MicroAmp® Fast Optical 96 well, Life Technologies Corporation, Carlsbad, CA, USA); the first forward and reverse primers of the gene of interest were introduced into each well for each case. The cDNA sample and the Master Mix with SYBR® green-based detection (Precision®PLUS qPCR Master Mix, Camberley, UK) were also placed on the multi-well plate. The StepOne Plus Real-Time PCR system (Applied Biosystems, Waltham, MA, USA) was used for amplification. Due to the low levels of viability (high toxicity) that occurred with high doses of BC, we studied the expression levels of pro-inflammatory cytokines (TNF-α and IL-1β) and caspase-3 with low doses of BC (1.5 μg/ml).

2.10. Quantification and statistical analysis

All the results shown in the text and in the figures were expressed as means ± standard error (SE) for each group. Significant differences ($p < 0.05$). Phagocytic activity was analyzed by a two-way ANOVA. The two factors considered for macrophages subjected to 1.5 or 150 μg/ml BC particles were radiation (radiated/non-radiated) X exposure time (24 or 72 h). The Bonferroni *t*-test for multiple comparisons was subsequently applied. Viability, nitric oxide, IL-1β, TNF-α and caspase 3 were analyzed by a one-way ANOVA. The Tukey test for multiple comparisons was subsequently applied. Natural logarithm transformations were applied to the data as needed to obtain normality and homoscedasticity.

All statistical analyses were performed with Sigma Plot 14.0 (Systat Software Inc., San Jose, CA, USA) and Grath Pad InStat. Culture data were obtained from at least four separate experiments and the values were normalized with respect to the control group values (100%).

3. Results

3.1. Cytotoxicity: cell viability analysis

To evaluate the combined cytotoxic effect of radiation and BC on RAW cells, we initially used the MTT assay. However, this test did not

Table 4
Primer sequences used for reverse transcription quantitative polymerase chain reaction (RT-qPCR).

	Primer	Accession number	Forward sequence (5′–3′)	Reverse sequence (5′–3′)
Mouse	TNF-α	NM_001278601.1	AGCCCCCAGTCTGTATCCTT	CTCCCTTTGCAGAACTCAGG
	Caspase 3	AC_125078.2	GGGCCTGTTGAAACTGAAAAA	CCGTCCTTTGAATTTCTCCA
	IL-1β	XM_006498795.4	AAGGAGACCAAGCAACGACAAAA	TGGGGACTCTGCAGACTCAAACT
	β-act	XM_03025405.7	AGCCATGTACGTAGCCATCC	CTCTCAGCTGTGGTGGTGAA

provide reliable viability results because the carbon particles interfered in a very significant way with the spectrophotometric identification of formazan. Carbon particle absorbance overlapped with the absorbance of the formazan produced by viable cells (see Supplementary material). Therefore, cell viability was analyzed using the Trypan Blue test.

The results indicated important alterations in the viability and cell proliferation of RAW cells from the combined effect of radiation and BC. The statistical analysis of cell viability by groups provided the following information:

- RAW cells did not show significant differences in cell viability when subjected to the simultaneous effect of BC 1.5 μg/ml and 24 h radiation, RAW BC 1.5 μg/ml + RAD (95.7 ± 2.04%) compared to the non-irradiated cell group (RAW-control), irradiated RAW-RAD (92.47 ± 3.2%) or incubated with BC RAW 1.5 μg/ml + non-RAD (98.18 ± 1.5%). See Fig. 1A.
- After 24 h radiation, the RAW cells subjected to the combined action of BC 150 μg/ml and radiation (BC150 μg/ml + RAD), with a viability of 37 ± 2% presented, significant differences with respect to the RAW-control, RAW-BC150 μg/ml + non-RAD, RAW-RAD ($p < 0.001$ in all cases). RAW-BC 150 μg/ml + non-RAD presented a cell viability of 67 ± 3.7%, with significant differences compared to control-RAW, RAW-RAD and/or the combined action RAW-BC 150 μg/ml + RAD ($p < 0.001$ in all cases). The RAW-RAD group did not show significant differences in viability compared to the RAW-control ($p \geq 0.05$). See Fig. 1C.
- When the radiation time increased to 72 h, RAW viability reduced drastically, decreasing in all groups, to 78.04 ± 0.6% in the RAW-BC 1.5 μg/ml + RAD, to 77.5 ± 2.5% in the RAW-RAD and 87 ± 0.6% in RAW-BC 1.5 μg/ml + no RAD with respect to RAW-control ($p < 0.001$, in all cases) See Fig. 1B.
- The combined effect RAW-BC 150 μg/ml + RAD caused intense toxicity, decreasing viability by up to 31 ± 1.06% with respect to the RAW-controls ($p < 0.001$). There was also a significant decrease in viability in RAW-BC 150 mg/ml + non-RAD to 52.5 ± 3.0% and in the RAW-RAD group to 77.5 ± 2.5% with respect to control-RAW ($p < 0.001$ in both cases). See Fig. 1D.

3.2. Combined effect of radiofrequency and black carbon on innate immune response

3.2.1. Phagocytic activity

The difference in the mean values for phagocytosis for the two levels of irradiation was statistically significant ($p = 0.039$) and greater than would be expected by chance after allowing for the effects of differences in radiation exposure time. A multiple comparison procedure was used to isolate the group(s) with significant differences.

The difference in the mean values for radiation exposure times was statistically significant ($p \leq 0.001$) and greater than would be expected by chance after allowing for effects of irradiation differences. A multiple comparison procedure was used to isolate the group(s) with significant differences. The effect of irradiation did not depend on radiation

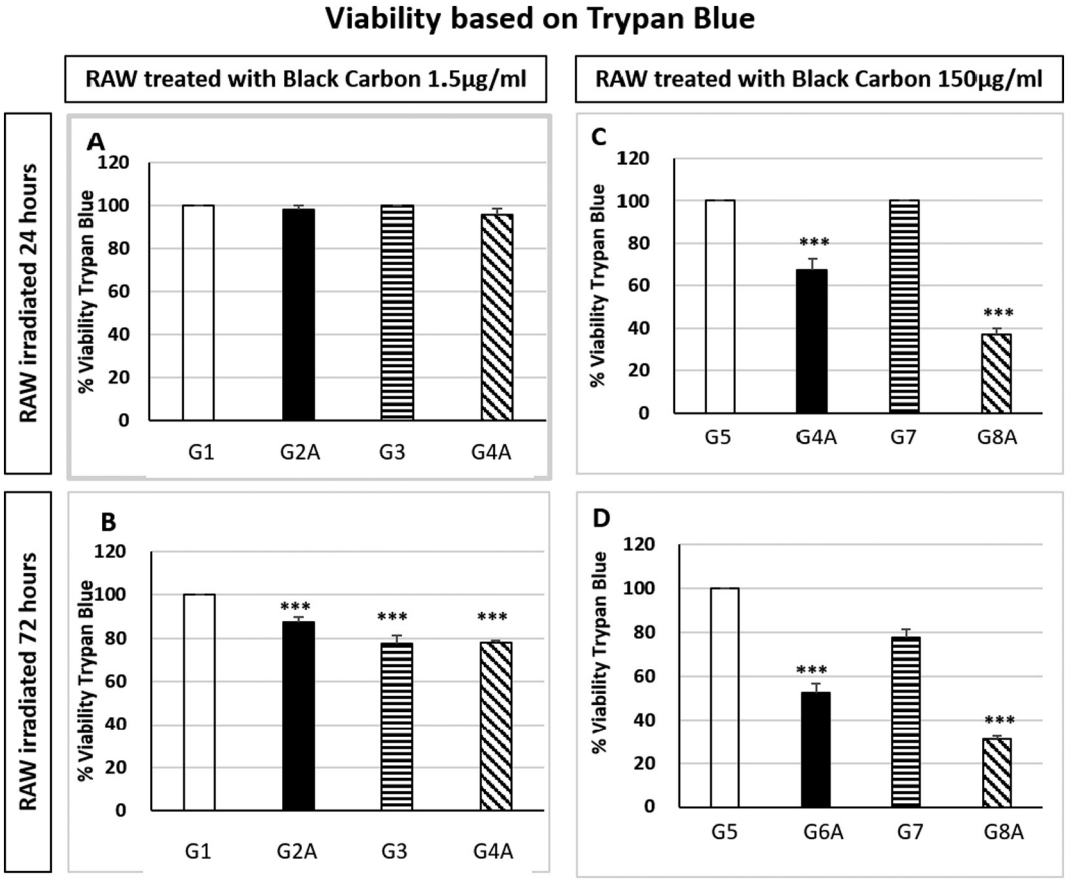


Fig. 1. Histograms showing the percentage of cell viability using Trypan blue: (A) group treated with BC 1.5 μg/ml and irradiated during 24 h; (B) group treated with BC 1.5 μg/ml and irradiated during 72 h; (C) group treated with BC 150 μg/ml and irradiated during 24 h; (D) group treated with BC 150 μg/ml and irradiated during 72 h. In G1 (RAW non-radiated 24 h), G2A (RAW BC 1.5 μg/ml + no RAD 24 h), G2B (RAW BC 150 μg/ml + no RAD 24 h), G3 (RAW RAD 24 h), G4A (RAW BC 1.5 μg/ml + RAD 24 h), G4B (RAW BC 150 μg/ml + RAD 24 h), G5 (RAW non-radiated 72 h), G6A (RAW BC 1.5 μg/ml + no RAD 72 h), G6B (RAW BC 150 μg/ml + no RAD 72 h), G7 (RAW RAD 72 h), G8A (RAW BC 1.5 μg/ml + RAD 72 h), G8B (RAW BC 150 μg/ml + RAD 72 h) groups. *** Indicates significant differences in relation to the non-radiated group ($p < 0.001$). Ninety-six samples were used, six for each group/time. Mean values are shown (six samples for each group/time). Error bars indicate the standard error of mean (SEM) within each group (radiated with/without BC, only BC or non-radiated). (For interpretation of the references to colour in this figure legend, the reader is referred to the web version of this article.)

exposure time (24 vs 72 h). There was no statistically significant interaction between irradiation and radiation exposure time ($p = 0.364$).

Phagocytic activity was increased in RAW cells treated with BC 1.5 μg + RAD 72 h compared to those treated with 1.5 μg + RAD 24 h ($p < 0.001$). However, there were also significant differences in non-RAD RAW treated with BC 1.5 μg at either 72 h or 24 h ($p < 0.001$). See Fig. 2A and Table 3A.

Phagocytosis increased with the effect of radiation in RAW-BC 1.5 μg + RAD (12.5 ± 1.5%) cells exposed to RF for 24 h compared to RAW-BC 1.5 μg + non-RAD (7.7 ± 1.4%) ($p = 0.04$). However, no significant differences in phagocytosis appeared between the RAW-BC 1.5 μg + RAD (22 ± 1%) and RAW-BC 1.5 μg + non-RAD (20 ± 1.7%) groups when the radiation was increased to 72 h ($p = 0.35$). See Fig. 2A, C (a,b) and Table 3A.

Differences in the mean values for phagocytosis at the different levels of irradiation was statistically significant ($p = 0.036$) and greater than would be expected by chance, after allowing for effects of differences in radiation exposure time. A multiple comparison procedure was used to isolate significantly different groups.

The difference in the mean values for phagocytosis at the different levels of radiation exposure time was not statistically significant ($p = 0.084$) or great enough to exclude the possibility that the difference was due to random sampling variability after allowing for the effects of differences in irradiation. The effect of different levels of

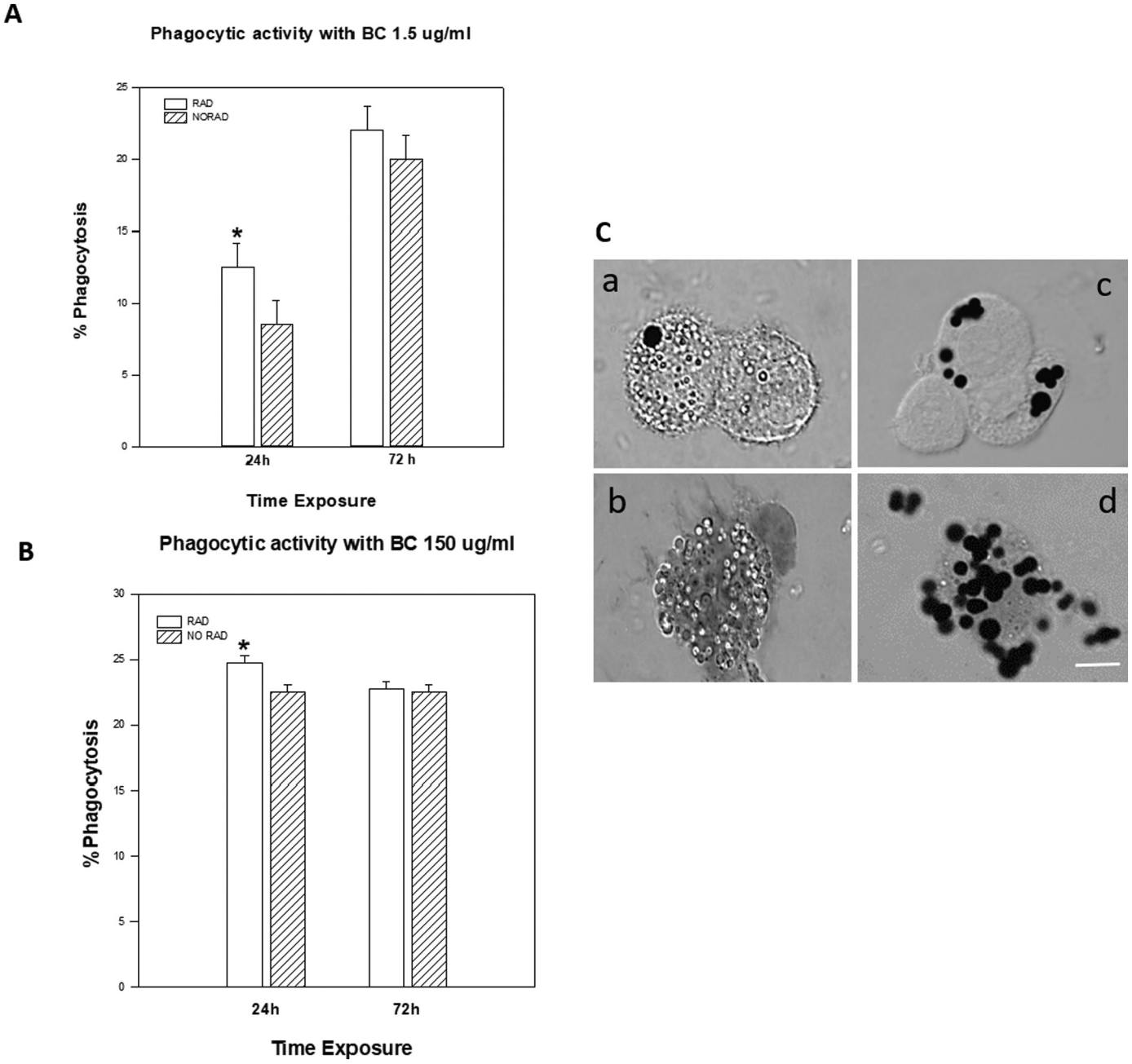


Fig. 2. Histograms showing the evolution of the phagocytosis rate (%) in 24/72 h: (A) phagocytic activity with BC 1.5 μg/ml; (B) phagocytic activity with BC 150 μg/ml. In (A) G2A (RAW BC 1.5 μg/ml + no RAD 24 h), G4A (RAW BC 1.5 μg/ml + RAD 24 h), G6A (RAW BC 1.5 μg/ml + no RAD 72 h), G8A (RAW BC 1.5 μg/ml + RAD 72 h) in (B) G2B (RAW BC 150 μg/ml + no RAD 24 h; G4B (RAW BC 150 μg/ml + RAD 24); G6B (RAW BC 150 μg/ml + no RAD 72 h), G8B (RAW BC 150 μg/ml + RAD 72 h) groups. * Indicates significant differences in relation to the non-radiated group ($p < 0.001$). Ninety-six samples were used, six for each group/time. Mean values are shown (six samples for each group/time). Error bars indicate the standard error of mean (SEM) within each group (radiated with/without BC, only BC or non-radiated); (C) microphotographs showing phagocytosis of BC particles in the macrophages, RAW BC 1.5 μg/ml + RAD 24 h (a) RAW BC 1.5 μg/ml + RAD 72 h (b) RAW BC 150 μg/ml + RAD 24 (c) RAW BC 150 μg/ml + RAD 72 h (d). Photographs taken at 100× magnification. Calibration bar 10 μm.

irradiation was not dependent on radiation exposure time. There was no statistically significant interaction between irradiation and radiation exposure time ($p = 0.084$). Phagocytic activity decreased significantly in RAW 150 μg/ml + RAD 24 h compared to RAW 150 μg/ml + RAD 72 h ($p = 0.021$). However, there were no statistically significant differences between the RAW + no-RAD treated with CB 150 μg/ml for 24 h and 72 h ($p = 0.7$). See Fig. 2A, C (c,d) and Table 3B.

Phagocytosis increased from the effect of radiation when RAW-BC 150 μg/ml + RAD (24.7 ± 0.25%) cells were exposed to RF for 24 h compared to RAW-BC 150 μg/ml + no-RAD (22.5 ± 0.6%) ($p = 0.011$). However, no significant differences in phagocytosis appeared between RAW-BC 150 μg/ml + RAD (22.7 ± 0.5%) and RAW-BC 150 μg/ml + non-RAD (22.5 ± 0–5%) when radiation time was increased to 72 h ($p = 0.745$). See Fig. 2A, C (c,d) and Table 3B.

3.2.2. Results of nitrite production

Twenty-four hours after radiation, nitrite values increased in cells that were irradiated 24 h and stimulated with LPS. However, nitrite

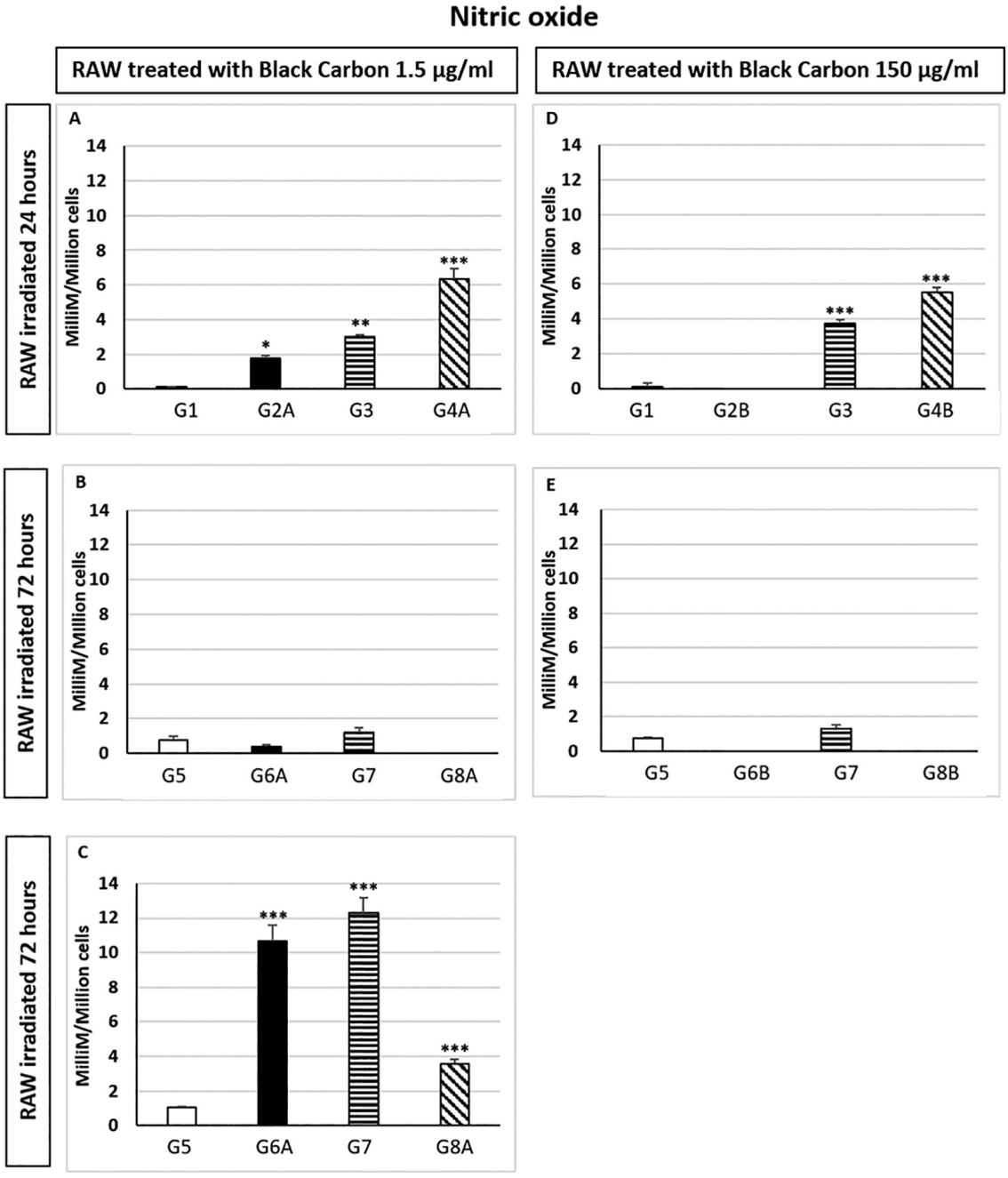


Fig. 3. Histograms showing nitric oxide concentration: (2A) nitric oxide concentrations at 24 h after RAW treatment with BC 1.5 μg/ml and irradiated during 24 h; (2B) nitric oxide concentrations at 24 h after RAW treatment with BC 1.5 μg/ml and irradiated during 72 h; (2C) nitric oxide concentrations at 72 h after RAW treatment with BC 1.5 μg/ml and irradiated during 72 h. (2D) Nitric oxide concentrations at 24 h after RAW treatment with BC 150 μg/ml and irradiated during 24 h; (2E) nitric oxide concentrations at 24 h after RAW treatment with BC 150 μg/ml and irradiated during 72 h in G1 (RAW non-radiated 24 h), G2A (RAW BC 1.5 μg/ml + no RAD 24 h), G2B (RAW BC 150 μg/ml + no RAD 24 h), G3 (RAW RAD 24 h), G4A (RAW BC 1.5 μg/ml + RAD 24 h), G4B (RAW BC 150 μg/ml + RAD 24 h), G5 (RAW non-radiated 72 h), G6A (RAW BC 1.5 μg/ml + no RAD 72 h), G6B (RAW BC 150 μg/ml + no RAD 72 h), G7 (RAW RAD 72 h), G8A (RAW BC 1.5 μg/ml + RAD 72 h), G8B (RAW BC 150 μg/ml + RAD 72 h) groups. Values were transformed based on percentage of viability for each group. Mean values are shown (six samples for each group/time). Error bars indicate the standard error of mean (SEM) within each group (radiated with/without BC, only BC or non-radiated). Significant differences in relation to the non-treated group are also shown:* ($p < 0.05$); ** ($p < 0.01$); *** ($p < 0.001$).

levels reached appreciable but lower values at 24 h when the RAW cells were irradiated 72 h and stimulated with LPS; the cells and increased nitrite values only recovered 72 h later when low doses of CB were used. Results from the one-way ANOVA and multiple comparisons with the Tukey test are as follows:

The highest nitrite levels were reached 24 h after stimulating RAW cells with LPS following exposure to radiation for 24 h.

When cell viability levels were higher (subgroups with BC 1.5 μg/ml) in the groups radiated for 24 h and subsequently stimulated with LPS for 24 h, the nitrite values were significantly higher (6.2 ± 0.6%) in the BC 1.5 μg/ml + RAD group compared to the rest of the groups ($p < 0.001$). Nitrite levels were halved in the RAW-RAD group (3 ± 0.13%) but were significantly higher ($p < 0.001$) than the RAW control (0.10 ± 0.5%) and BC 1.5 μg/ml + non-RAD (1.66 ± 0.20). Seventy-two hours after stimulation with LPS following 24 h radiation, there was a considerable decrease in the levels of nitric oxide, which was only detectable in the RAW-RAD and BC 1.5 μg/ml + no RAD groups (0.92 ± 0.30% and 0.34 ± 0.10% respectively) and not significantly different from the control – RAW or BC 1.5 μg/ml + RAD ($p > 0.05$). See Fig. 3A.

There was, however, a recovery in nitrite production when this subset of cells (with BC 1.5 μg/ml) were irradiated for 72 h and stimulated with LPS for an additional 72 h. The RAW-RAD and RAW-BC 1.5 μg/ml + no-RAD (9.54 ± 0.90% and 9.35 ± 0.90%) groups reached very similar levels and were significantly different from the RAW control group ($p < 0.001$). Finally, the RAW-BC 1.5 μg/ml + RAD group presented significant differences with respect to the RAW-RAD and RAW-BC groups ($p < 0.001$ in both cases) but did not reach nitrite values that were significantly different to the RAW-control ($p > 0.05$). See Fig. 3B, C.

When cellular toxicity levels were high (subgroups with BC 150 μg/ml), nitrite values were significantly higher (3.75 ± 0.07%) in the RAW-RAD group compared to the RAW-control, the BC + non-RAD and the BC150 μg/ml + RAD groups ($p < 0.001$). In the BC 150 μg/ml + RAD group, 24-hour stimulation with LPS following 24-hour radiation significantly increased nitrite values, which reached 2.06 ± 0.0% picomoles in relation to the control-RAW and RAW-RAD groups ($p < 0.001$). Finally, in the BC 150 μg/ml + non-RAD group, 24-hour LPS stimulation did not induce appreciable levels of nitrites, nor were nitrites detectable after 72 h of LPS stimulation following 24 h radiation. See Fig. 3D.

RAW cells irradiated for 72 h and stimulated with LPS produced no detectable nitrite levels at 24 h. However, when cells were stimulated for 72 h, nitrite levels were detectable but lower than with 24 h radiation in all groups except the control – RAW. Similarly, nitrite was

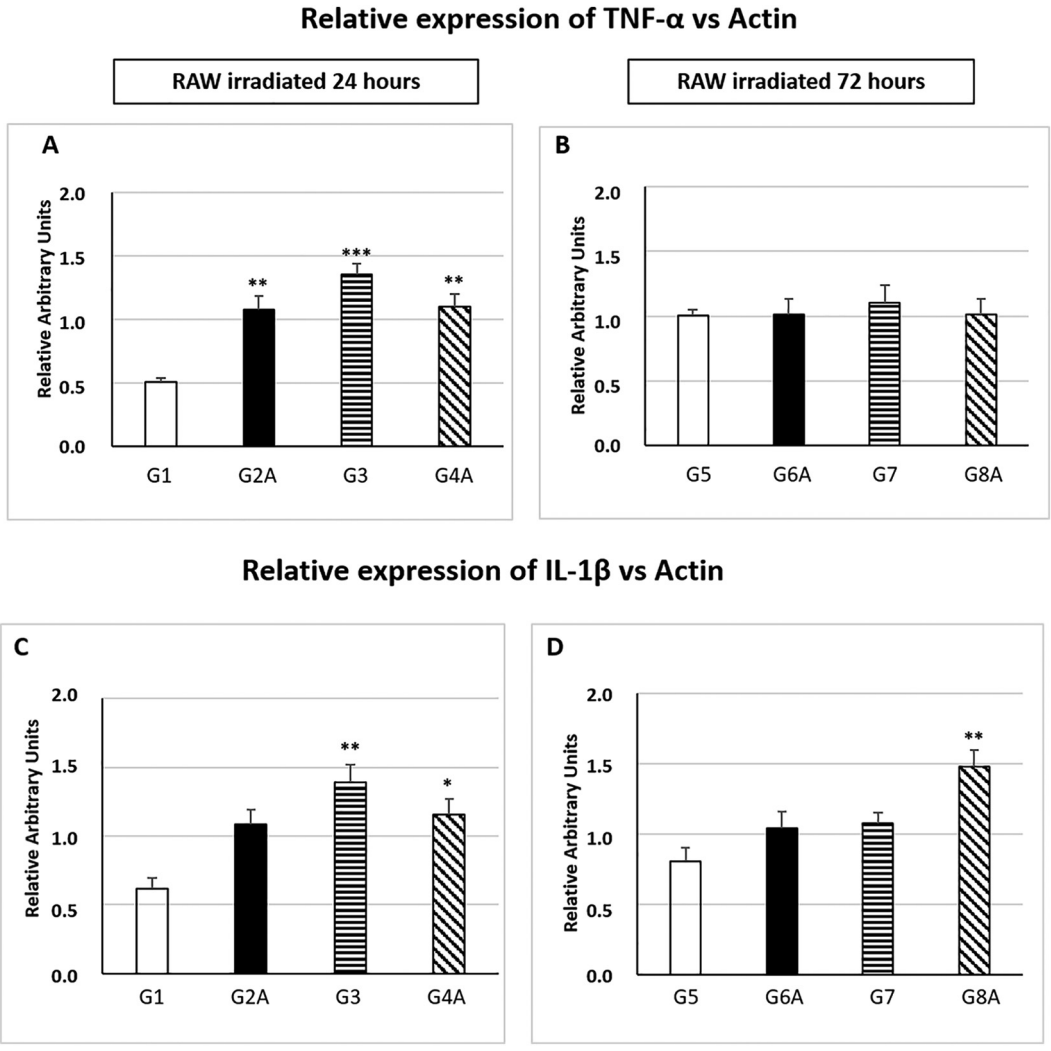


Fig. 4. Histograms of mRNA expression of TNF-α (A and B) and IL-1β (C and D) protein. (4A; 4C) RAW treated 24 h. (4B; 4D) RAW treated 72 h in G1 (RAW non-radiated 24 h), G2A (RAW BC 1.5 μg/ml + no RAD 24 h), G3 (RAW RAD 24 h), G4A (RAW BC 1.5 μg/ml + RAD 24 h), G5 (RAW non-radiated 72 h), G6A (RAW BC 1.5 μg/ml + no RAD 72 h), G7 (RAW RAD 72 h), G8A (RAW BC 1.5 μg/ml + RAD 72 h) groups. Mean values are shown (six samples for each group/time). Error bars indicate the standard error of mean (SEM) within each group (radiated with/without BC, only BC or non-radiated). Significant differences in relation to the non-treated group are also shown:* ($p < 0.05$); ** ($p < 0.01$); *** ($p < 0.001$).

detectable at 24 h in the RAW cell groups that had been stimulated with LPS and subjected to 72 h radiation. Again, RAW-RAD had highest nitrite levels (1 ± 0.23%) but did not present significant differences in relation to control-RAW ($p > 0.05$). See Fig. 3E.

3.2.3. Proinflammatory factors

3.2.3.1. TNF_{α}. Twenty-four hours after radiation exposure, inflammatory activity was measured through tumor necrosis factor alpha. Levels in the RAW-RAD group (1.34 ± 0.14%), in the RAW-BC + RAD group (1.09 ± 0.10%) and in the RAW-BC 1.5 μg/ml + non-RAD group (1.07 ± 0.10%) were significantly higher than in the control-RAW group (0.5 ± 0.03%) ($p < 0.001$, $p < 0.01$ and $p < 0.01$, respectively). However, 72 h after radiation, no significant differences were found with respect to the control ($p > 0.05$) in any of the groups studied. See Fig. 4A and B.

3.2.3.2. IL-1β. Twenty-four hours after radiation exposure, inflammatory activity measured through interleukin-1β levels again reached significantly higher values in the RAW-RAD (1.38 ± 0.13%) and RAW-BC 1.5 μg/ml + RAD (1.15 ± 0.12%) groups compared to RAW-control (0.6 ± 0.08%) ($p < 0.01$, $p < 0.05$) respectively. The RAW BC 1.5 μg/ml + no-RAD group (1.08 ± 0.01%) did not show significant differences with respect to the control ($p > 0.05$).

Seventy-two hours after radiation, however, only the RAW BC group 1.5 μg/ml + RAD 72 h had significantly high levels (1.47 ± 0.12%) compared to the RAW-control group (0.8 ± 0.10%) ($p < 0.01$). See Fig. 4C and D.

3.3. Combined effect of radiofrequency and black carbon on apoptosis

Twenty-four hours after radiation, the combined action of RF and BC particles significantly increased the caspase-3 values in the RAW-BC 1.5 μg/ml + RAD (1.51 ± 0.1%) and RAW-RAD (1.36 ± 0.1%) groups with respect to the RAW-control (0.81 ± 0.8%) ($p < 0.01$, $p < 0.05$). However, in the RAW-BC + non-RAD group (1.09 ± 0.1%), caspase-3 values were not significantly compared to the RAW-control ($p > 0.05$).

Seventy-two hours after radiation, there were still significant differences in caspase-3 levels between the RAW-BC 1.5 + RAD group (1.24 ± 0.97%) and the RAW-control group (0.84 ± 0.07%) ($p < 0.05$). See Fig. 5.

4. Discussion

In this study, we demonstrated that exposure of the RAW cell line to RF at 2.45 GHz increased the toxicity associated with BC by activating the pro-apoptotic response of caspase-3 and the pro-inflammatory responses of TNF-α and interleukin-1β in the macrophages. The combined effect of non-ionizing radiation in the RAW cells exposed to fine and coarse black carbon BC prolonged phagocytic activity and the production of NO in macrophages previously induced through stimulation with LPS bacterial endotoxin.

Until now, in vitro experimental evidence of the mutual or synergic interaction between different kinds of phenomena, one electromagnetic (2.45 GHz RF) and the other chemical (BC environmental particulate matter) had not been found. In the only known relevant study on a human cell line of monocytes, the authors concluded that exposure to RF alone or in combination with ultra-fine particles (UFP) did not interfere with stress-related responses (Simko et al., 2006).

Most of the studies cited in the bibliography concern research on the repercussions on human and/or animal health from environmental particulate matter (Niranjan and Thakur, 2017) or RF (Pall, 2018) separately. In prior studies, we found that the interaction of RF at 2.45 GHz alone or combined with 900 MHz in the RAW cells provoked dysfunction in the inflammatory response and diminished immune system functioning (López-Furelos et al., 2018). In this experimental work, which incorporated a chemical environmental agent, we found that non-ionizing radiation associated with environmental particles can affect the mechanisms that alter cellular functioning and immune response (Lawal, 2018).

Results from diverse in vitro experimental models indicate that RF can have bio-effects and affect cell viability, depending on the cell type (Wójcik-Piotrowicz et al., 2014) and the electromagnetic parameters applied, such as frequency (Saliev et al., 2019) and exposure time (García-Minguillán López et al., 2019). In the present work, toxicity increased clearly when the two environmental pollutants (BC + RF) acted jointly, compared to the sole action of RF. In the RAW-BC macrophages, toxicity increased significantly

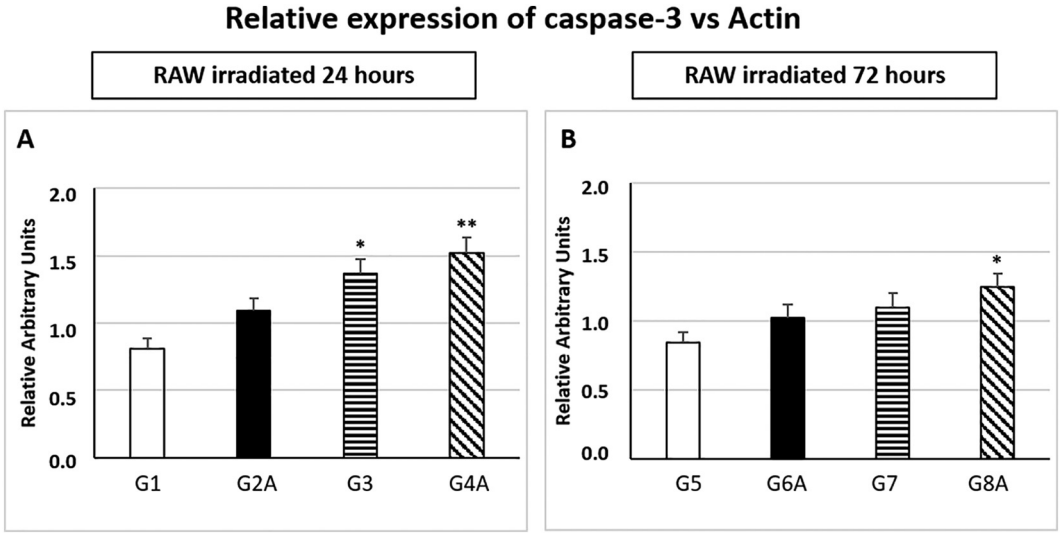


Fig. 5. Histograms of mRNA expression of caspase-3 protein (5A) RAW treated 24 h. (5B) RAW treated 72 h in G1 (RAW non-radiated 24 h), G2A (RAW BC 1.5 μg/ml + no RAD 24 h), G3 (RAW RAD 24 h), G4A (RAW BC 1.5 μg/ml + RAD 24 h), G5 (RAW non-radiated 72 h), G6A (RAW BC 1.5 μg/ml + no RAD 72 h), G7 (RAW RAD 72 h), G8A (RAW BC 1.5 μg/ml + RAD 72 h) groups. Mean values are shown (six samples for each group/time). Error bars indicate the standard error of mean (SEM) within each group (radiated with/without BC, only BC or non-radiated). Significant differences in relation to the non-treated group are also shown:* ($p < 0.05$); ** ($p < 0.01$).

compared to RAW-RAD (Fig. 1C, D). Black carbon PM is known to cause toxicity (Wang et al., 2014) and premature human mortality (Goto, 2014) in urban areas (Thomson et al., 2015). However, our findings indicate that the toxicity caused by BC in the RAW-BC + no RAD group was significantly lower than that of the RAW-BC + RAD group after 24 or 72 h exposure (Fig. 1C). These data inform that each toxic agent (RF or BC) had damaging effects as an individual stressor and combining them generated substantially different results (Kostoff et al., 2018). The fact that very low doses of BC (1.5 μg/ml), when combined with RF, significantly decreased macrophage viability suggests that simultaneous action increased toxicity (Kostoff et al., 2018; Kostoff and Lau, 2017, 2013; Juutilainen, 2008) (Fig. 1B). Thus, there is a decrease in the levels of each toxic agent associated with damage, when compared to the levels of each of the constituents separately. Accordingly, we propose the existence of an RF-dependent mechanism that modulates cellular viability and the efficacy of cell death (Wójcik-Piotrowicz et al., 2017).

The RAW 264.7 macrophage cell line can be activated by external biological stimuli such as the Gram negative (−) bacterial endotoxin LPS (Stuehr and Marletta, 1987, 1985), by physical stimuli such as one or two RF signals (López-Furelos et al., 2018) or by chemical stimuli such as BC environmental particulate matter (Gawda et al., 2018; Schins et al., 2004), provoking an inflammatory response involving the liberation of NO in the immune cells. Our findings coincide with those of other authors, who reported that the NO inflammatory response tripled when the effect of electromagnetic fields was combined with non-toxic doses of LPS (Pilla, 2012) and reached maximum nitrite levels from stimulation after 24 h, when the macrophages were simultaneously exposed to BC and LPS (Gawda et al., 2018). The most novel findings of this study indicate that NO levels under cellular stimulation from LPS for 24 h (after 24 h of radiation) doubled significantly in the RAW-BC 1.5 μg/ml + RAD group with respect to the values of the radiated macrophages (RAW-RAD) and/or tripled significantly with respect to the nitrite values for the macrophages exposed to BC or the RAW-control groups (Fig. 3A). Radiation must have acted to increase the induction of NO even when the viability levels of the macrophages were low (Fig. 1D), causing exhaustion of the cellular machinery 48 h after exposure to RF, despite the combined toxicity. Some authors have suggested that electromagnetic fields could act initially as first messengers, modulating the NO signaling pathways dependent on Ca-Calmodulin (Pall, 2018). To this we add evidence that RF acting in combination with BC particles prolongs by 24 h the macrophage cellular inflammatory functions associated with NO (Fig. 3A, D).

One of the crucial functions of macrophages is phagocytic activity, which in this study was substantially modified by the effect of both environmental agents, especially radiation (Fig. 2A, B). Some authors suggest an important increase in the cellular response from the effects of radiation that is similar to chemical stimuli (Frahm et al., 2006; Simkó et al., 2001). Others suggest the opposite: a decrease in phagocytic activity due to the interaction of one or two RF (López-Furelos et al., 2018) or the action of magnetic fields (Tenuzzo et al., 2006). Different exposure conditions and pre-stimulation of the cells might explain such contradictory data (Dini, 2010). Electromagnetic fields can alter proteins in the plasmatic membrane, the cytoskeleton, distorting the ionic channels (especially $[Ca^{2+}]$) and interfering with physiological processes such as phagocytosis (Dini and Abbro, 2005; Rosen, 2003).

It is a known fact that environmental particulate matter generated by incomplete combustion of diesel, which is mainly composed of carbon (Vedal et al., 2013), provoke the activation and dysfunction of macrophages (Lawal, 2018). During phagocytosis of the BC particles, determining the number of particles internalized by the macrophage cells is useful for evaluating the levels of toxicity produced after exposure (Clift et al., 2008). Accurate measurement of internalized particles requires distinguishing completely engulfed particles from those that have adhered to the membrane (Leclerc et al., 2010). This experimental work included phagocytes in different phases of phagocytosis: from the initial phase of particles adhering to the macrophages to the final internalization of the particles inside the RAW 264.7 cells (Rosales and Uribe-Querol, 2017). We estimated the rate of phagocytosis in macrophages in different phases of phagocytosis (López-Furelos et al., 2018; Kiama et al., 2001) (Fig. 2A, B, C and D). The study was done 24 or 72 h after exposure, which allowed us to interpret the immune response and early phagocytosis in association with toxic agents (Lee et al., 2017). Related to this process, some authors indicate that the nitrite ions generated by the activated macrophages play an important role in phagosome implementation (Zagryazhskaya et al., 2010). There is a series of data that could indicate a slowing or prolonging of macrophage phagocytic functions, since phagocytosis levels were elevated 24 h after radiation, in contrast with maximum nitrite levels obtained 48 h later (24 h after finishing radiation). However, it should be kept in mind that in vitro environmental studies with environmental particulate matter often report that the largest particles are the most particles are also the most toxic and inflammatory (Guastadisegni et al., 2010; Schwarze et al., 2007). Other data that contributes experimental evidence to our hypothesis indicate that the coarse particles found within the experimental range of this in vitro study might exercise their pro-inflammatory effect by modulating intra-cellular signaling of calcium in the macrophages. This leads to increased expression of pro-inflammatory cytokines, which also alter phagocytic capacity (Brown et al., 2004). RF could retard some active biological processes of the macrophage, interfering with the cellular signaling that initiates important functions of this immune cell (Dini, 2010). The immediate immune capacities of the RAW cells are modulated by RF, as we saw in the genetic expression after 24 h of pro-inflammatory factors TNFα and IL-1β from interaction with particulate matter (Cho et al., 2018) (4A, 4C). The inflammatory capacity of cytokines affected by environmental pollution involving coarse/fine particles is established by a range of factors: concentration mass (Grahame and Schlesinger, 2007; Nel, 2005), physical-chemical characteristics (Brown et al., 2001), capacity to provoke oxidative stress (Ayres et al., 2008), and the capacity of the bacterial endotoxin LPS to provoke innate immune responses (Schins et al., 2004; Osornio-Vargas et al., 2003). Despite notions of a kind of feedback that regulates between the inflammatory effect of the cytokines and NO (Nemoto et al., 1999) or vice-versa (Wu et al., 2003), this effect cannot be attributed to the intervention of LPS (West et al., 1994) since in this in vitro model it was only used to stimulate NO and not for the cytokines. It rather clearly points to independent effects or mechanisms, though both pathways are mutually modulated. The highest levels of TNF-α and interleukin-1β were produced exclusively by RF (RAW-RAD) interaction with the plasmatic membrane (Eichwald and Kaiser, 1995), probably due to a voltage-dependent increase in the extracellular calcium channels (Cho et al., 1999), intra-cellular calcium deposits (Ross et al., 2016), or transfer of the charge to the DNA (Blank and Goodman, 2008). The stimulus of environmental particles in the RAW-BC + no-RAD group induced significantly inferior levels of interleukins that were dependent on intra-cellular calcium (Brown et al., 2002) or not dependent on calcium (Sakamoto et al., 2007). The combination of both stress factors at 24 h did not provoke an additive or synergic response of interleukin-1β, which is continuously induced depending on the power of the stimulus and the extra-cellular requirement (López-Castejón and Brough, 2011), and which reached its highest concentration after 72 h from the interaction of both stimuli.

In certain stress situations, caspase-3 and the tumor necrosis factor alpha, together with interleukin-1β can induce apoptotic cellular death (Chanana et al., 2007). Thus, the MAP kinase (MAPK) ERK1/K2 signal transduction pathway can function in a pro-apoptotic way (Lu and Xu, 2006) by neutralizing the TNFα that regulates apoptosis (Wallach et al., 1999), induced by the stimulus of particulate matter (Chin et al., 1998) or radiation (Park et al., 1999; Kitagawa et al., 2002). In this in vitro model the TNF-α were no longer significant at 72 h, indicating the absence of the anti-apoptotic effect from the

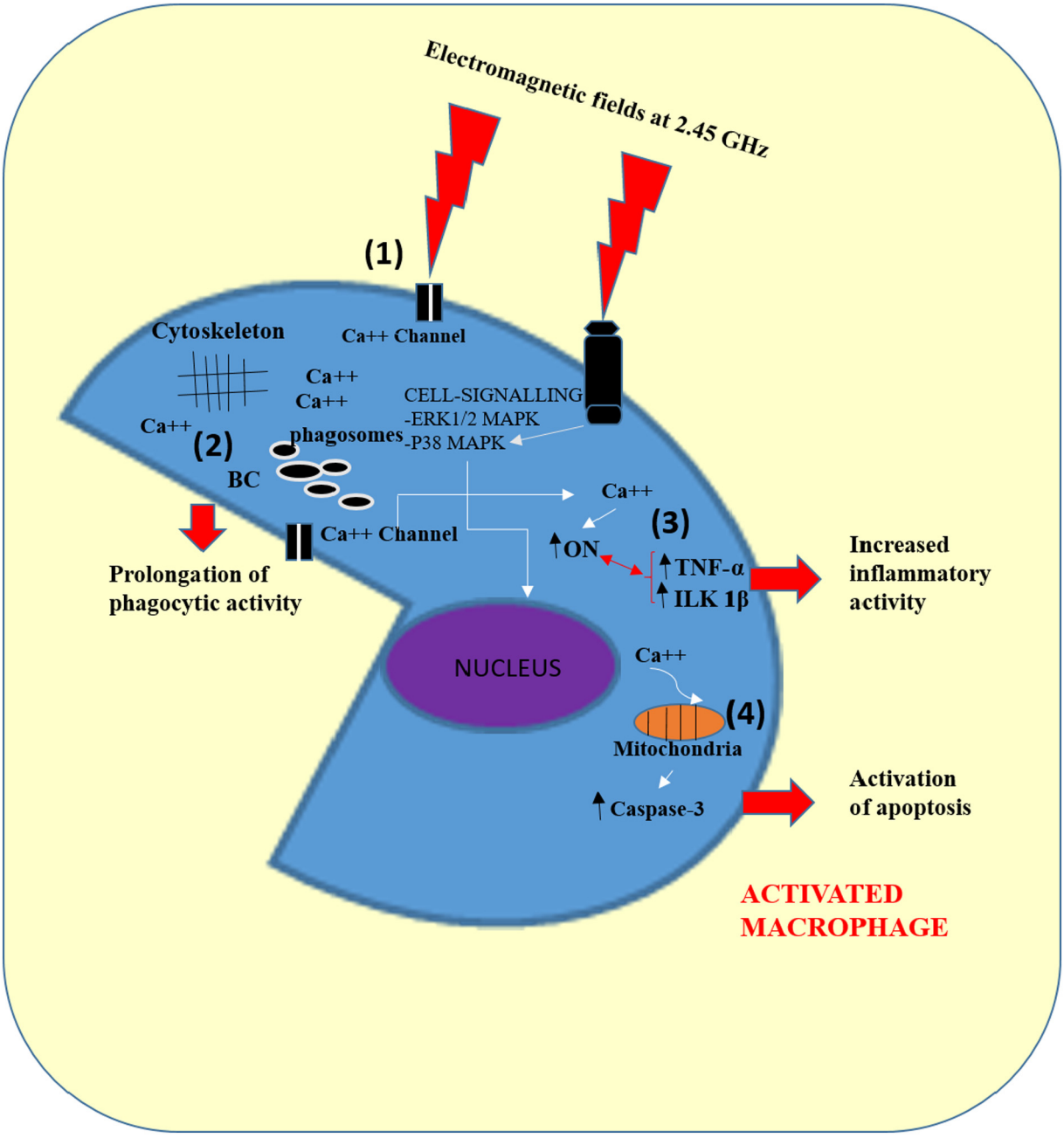


Fig. 6. Illustrations explaining the hypothesis of the mechanism by which RF at 2.45 GHz and the Black Carbon (BC) in the activated macrophage would act in combination. (1) RF and BC stimulate the ion channels [Ca2 +] and facilitate the entry of the ion at the intracytoplasmic level (2), causing alteration of the cytoskeleton and prolongation of phagocytic activity (3) along with increased inflammatory activity and release of NO, TNF-α and interleukin 1β, (4) which activates the apoptosis cascade by increasing caspase-3.

inhibition of ERK1/K2 or prolonged stimulation (Lu et al., 2002). For its part, interleukin-1β activates numerous transduction signals through kinase proteins that are activated by stress, such as p38 mitogen-activated protein kinase (MAPK) (Bankers-Fulbright et al., 1996) and intervene during exposure to both ELF and RF (Leszczynski et al., 2004, 2002). The anti-apoptotic effect of ERK1/K2 can also be indirectly regulated by the p38 signal (Li et al., 2003; Liu and Hofmann, 2004). Activation of ERK1/K2 in response to harmful stimuli in the DNA clearly promotes cellular apoptosis by improving the activity of some pro-apoptotic signaling molecules (Lu and Xu, 2006). The synergic effect of RF and BC could provoke activation of ERK1/K2 and pro-apoptotic subfamily BAX/BAK in macrophages, unleashing the activation of interleukin-1β and caspase-3 (Vince et al., 2018). This fact would indicate that alterations in macrophage cellular function could be modified by apoptosis-related gene expression, which regulates the transduction of multiple signaling pathways (Tenuzzo et al., 2009) (Fig. 6).

5. Conclusions

Toxicity in the RAW macrophage cell line increased dramatically, along with pre-apoptotic activation of caspase-3 when non-ionizing radiation interacted with BC particles. Prolonged phagocytosis and amplification of the macrophage inflammatory response could play an important part in the interaction of RF in the macrophage membrane and cytoplasm, exercising a voltage-dependent modulation (Pall, 2018; Pilla, 2012; Cho et al., 1999; Ross et al., 2016) on cellular machinery that has been altered by the effect of BC particulate matter (Brown et al., 2002; Sakamoto et al., 2007). In the macrophage cells activated

by both stimuli, intracellular signaling pathways acted to unleash anti-apoptotic or pre-apoptotic mechanisms that eventually provoked exhaustion and premature death of these immune cells. More in-depth study is needed to better understand the repercussions of both environmental agents in the immune response and their potential influence on the induction and/or aggravation of human autoimmune and inflammatory illnesses.

CRediT authorship contribution statement

Rosa Ana Sueiro-Benavides: Methodology, Validation, Formal analysis, Investigation, Data curation, Writing - original draft, Writing - review & editing, Supervision. **Jose Manuel Leiro-Vidal:** Methodology, Investigation, Resources, Supervision. **Aarón Ángel Salas-Sánchez:** Methodology, Software, Visualization, Supervision. **J. Antonio Rodríguez-Gonzalez:** Software, Visualization, Supervision. **Francisco J. Ares-Pena:** Conceptualization, Resources, Supervision, Project administration, Funding acquisition. **M. Elena López Martín:** Conceptualization, Methodology, Validation, Formal analysis, Investigation, Data curation, Writing - original draft, Writing - review & editing, Supervision, Project administration, Funding acquisition.

Declaration of competing interest

The authors declare that they have no known competing financial interests or personal relationships that could have appeared to influence the work reported in this paper.

Acknowledgments

The authors wish to thank Rafael Fuentes for his help and technical assistance.

Funding

This work was supported in part by the FEDER/Ministerio de Ciencia, Innovación y Universidades-Agencia Estatal de Investigación under Project TEC2017-86110-R. The work of A.A.S.-S. is supported by the Xunta de Galicia Postdoctoral Fellowship, reference ED481/008.

Appendix A. Supplementary data

Supplementary data to this article can be found online at https://doi.org/10.1016/j.scitotenv.2020.142681.

References

Adams, D.D., Knight, J.G., Ebringer, A., 2010. Autoimmune diseases: solution of the environmental, immunological and genetic components with principles for immunotherapy and transplantation. Autoimmun. Rev. 9, 525–530. https://doi.org/10.1016/j.autrev.2009.12.012.

Anaya, J.M., 2012. Common mechanisms of autoimmune diseases (the autoimmune tautology). Autoimmun. Rev. 11, 781–784. https://doi.org/10.1016/j.autrev.2012.02.002.

Ayres, J.G., Borm, P., Cassee, F.R., Castranova, V., Donaldson, K., Ghio, A., Harrison, R.M., Hider, R., Kelly, F., Kooter, I.M., Marano, F., Maynard, R.L., Mudway, I., Nel, A., Sioutas, C., Smith, S., Baeza-Squiban, A., Cho, A., Duggan, S., Froines, J., 2008. Evaluating the toxicity of airborne particulate matter and nanoparticles by measuring oxidative stress potential - a workshop report and consensus statement. Inhal. Toxicol. 20, 75–99. https://doi.org/10.1080/08958370701665517.

Bankers-Fulbright, J.L., Kalli, K.R., McKean, D.J., 1996. Interleukin-1signal transduction. Life Sci. 59, 61–83. https://doi.org/10.1016/0024-3205(96)00135-X.

Belyaev, I., Dean, A., Eger, H., Hubmann, G., Jandrisovits, R., Kern, M., Kundi, M., Moshammer, H., Lercher, P., Müller, M., Oberfeld, G., Ohnsorge, P., Pelzmann, P., Scheingraber, C., Thill, R., 2016. EUROPAEM EMF guideline 2016 for the prevention, diagnosis and treatment of EMF-related health problems and illnesses. Rev. Environ. Health 31, 363–397. https://doi.org/10.1515/reveh-2016-0011.

Blank, M., Goodman, R., 2008. A mechanism for stimulation of biosynthesis by electromagnetic fields: charge transfer in DNA and base pair separation. J. Cell. Physiol. 214, 20–26. https://doi.org/10.1002/jcp.21198.

Brown, D.M., Wilson, M.R., MacNee, W., Stone, V., Donaldson, K., 2001. Size-dependent proinflammatory effects of ultrafine polystyrene particles: a role for surface area and oxidative stress in the enhanced activity of ultrafines. Toxicol. Appl. Pharmacol. 175, 191–199. https://doi.org/10.1006/taap.2001.9240.

Brown, D.M., Donaldson, K., Stone, V., 2002. Role of calcium in the induction of TNFα expression by macrophages on exposure to ultrafine particles. Ann. Occup. Hyg. 46, 219–222. https://doi.org/10.1093/annhyg/mef674.

Brown, D.M., Donaldson, K., Stone, V., 2004. Effects of PM10 in human peripheral blood monocytes and J774 macrophages. Respir. Res. 5, 29. https://doi.org/10.1186/1465-9921-5-29.

Chanana, V., Majumdar, S., Rishi, P., 2007. Involvement of caspase-3, lipid peroxidation and TNF-alpha in causing apoptosis of macrophages by coordinately expressed Salmonella phenotype under stress conditions. Mol. Immunol. 44, 1551–1558. https://doi.org/10.1016/j.molimm.2006.08.022.

Chin, B.Y., Choi, M.E., Burdick, M.D., Strieter, R.M., Risby, T.H., Choi, A.M., 1998. Induction of apoptosis by particulate matter: role of TNF-α and MAPK. Am. J. Phys. 275, L942–L949. https://doi.org/10.1152/ajplung.1998.275.5.L942.

Cho, M.R., Thatte, H.S., Silvia, M.T., Golan, D.E., 1999. Transmembrane calcium influx induced by ac electric fields. FASEB J. 13, 677–683. https://doi.org/10.1096/fasebj.13.6.677.

Cho, C.C., Hsieh, W.Y., Tsai, C.H., Chen, C.Y., Chang, H.F., Lin, C.S., 2018. In vitro and in vivo experimental studies of PM (2.5) on disease progression. Int. J. Environ. Res. Public Health 15, 1380. https://doi.org/10.3390/ijerph15071380.

Clift, M.J., Rothen-Rutishauser, B., Brown, D.M., Duffin, R., Donaldson, K., Proudfoot, L., Guy, K., Stone, V., 2008. The impact of different nanoparticle surface chemistry and size on uptake and toxicity in a murine macrophague cell line. Toxicol. Appl. Pharmacol. 232, 418–427. https://doi.org/10.1016/j.taap.2008.06.009.

Deweirdt, J., Quignard, J.F., Lacomme, S., Gontier, E., Mornet, S., Savineau, J.P., Marthan, R., Guibert, C., Baudrimont, I., 2020. In vitro study of carbon black nanoparticles on human pulmonary artery endothelial cells: effects on calcium signaling and mitochondrial alterations. Arch. Toxicol. 97, 2331–2348. https://doi.org/10.1007/s00204-020-02764-9.

Dini, L., 2010. Phagocytosis of dying cells: influence of smoking and static magnetic fields. Apoptosis 15, 1147–1164. https://doi.org/10.1016/j.taap.2008.06.009.

Dini, L., Abbro, L., 2005. Bioeffects of moderate-intensity static magnetic fields on cell cultures. Microm. 36, 195–217. https://doi.org/10.1016/j.micron.2004.12.009.

Eichwald, C., Kaiser, F., 1995. Model for external influences on cellular signal transduction pathways including cytosolic calcium oscillations. Bioelectromagnetics 16, 75–85. https://doi.org/10.1002/bem.2250160203.

Frahm, J., Lantow, M., Lupke, M., Weiss, D.G., Simkó, M., 2006. Alteration in cellular functions in mouse macrophages after exposure to 50 Hz magnetic fields. J. Cell. Biochem. 99, 168–177. https://doi.org/10.1002/jcb.20920.

García-Minguillán López, O., Jiménez Valbuena, A., Maestú Unturbe, C., 2019. Significant cellular viability dependence on time exposition at ELF-EMF and RF-EMF in vitro studies. Int. J. Environ. Res. Public Health 16, 2085. https://doi.org/10.3390/ijerph16122085.

Gawda, A., Majka, G., Nowak, B., Śróttek, M., Walczewska, M., Marcinkiewicz, J., 2018. Air particulate matter SRM 1648a primes macrophages to hyperinflammatory response after LPS stimulation. Inflamm. Res. 67, 765–776. https://doi.org/10.1007/s00011-018-1165-4.

Goto, D., 2014. Modeling of black carbon in Asia using a global-to-regional seamless aerosol-transport model. Environ. Pollut. 195, 330–335. https://doi.org/10.1016/j.envpol.2014.06.006.

Grahame, T.J., Schlesinger, R.B., 2007. Health effects of airborne particulate matter: do we know enough to consider regulating specific particle types or sources? Inhal. Toxicol. 19, 457–481. https://doi.org/10.1080/08958370701382220.

Guastadisegni, C., Kelly, F.J., Cassee, F.R., Gerlofs-Nijland, M.E., Janssen, N.A.H., Pozzi, R., Brunekreef, B., Sandström, T., Mudway, I., 2010. Determinants of the proinflammatory action of ambient particulate matter in immortalized murine macrophages. Environ. Health Perspect. 118, 1728–1734. https://doi.org/10.1289/ehp.1002105.

Hiraiwa, K., Van Eeden, S.F., 2013. Contribution of lung macrophages to the inflammatory responses induced by exposure to air pollutants. Mediat. Inflamm. 10, 619523. https://doi.org/10.1080/08958370701382220.

Jalava, P.I., Hirvonen, M.R., Sillanpää, M., Pennanen, A.S., Happo, M.S., Hillamo, R., Cassee, F.R., Gerlofs-Nijland, M., Borm, P.J.A., Schins, R.P.F., Janssen, N.A.H., Salonen, R.O., 2009. Associations of urban air particulate composition with inflammatory and cytotoxic responses in RAW 246.7 cell line. Inhal. Toxicol. 21, 994–1006. https://doi.org/10.1080/08958370802695710.

Jing, A., Qian, Z., Meiying, W., Lu, W., Yufang, Z., Jialiang, F., Yu, S., Yingjun, C., 2019. Interactions between oxidative stress, autophagy and apoptosis in A549 cells treated with aged black carbon. Toxicol. In Vitro 54, 67–74. https://doi.org/10.1016/j.tiv.2018.09.008.

Juutilainen, J., 2008. Do electromagnetic fields enhance the effects of environmental carcinogens? Radiat. Prot. Dosim. 132, 228–231. https://doi.org/10.1093/rpd/ncn258.

Kiama, L., Cochand, L., Karlsson, L.P., Gehr, N.P., 2001. Evaluation of phagocytic activity in human monocyte-derived dendritic cells. J. Aerosol Med. 14, 289–299. https://doi.org/10.1089/089426801316970240.

Kitagawa, D., Tanemura, S., Ohata, S., Shimizu, N., Seo, J., Nishitai, G., Watanabe, T., Nakagawa, K., Kishimoto, H., Wada, T., Tezuka, T., Yamamoto, T., Nishina, H., Katada, T., 2002. Activation of extracellular signal-regulated kinase by ultraviolet ismediated through src-dependent epidermal growth factor receptorphosphorylation. Its implication in an anti-apoptotic function.J. Biol. Chem. 277, 366–371. https://doi.org/10.1074/jbc.M107110200.

Kostoff, R.N., Lau, C.G.Y., 2013. Combined biological and health effects of electromagnetic fields and other agents in the published literature. Technol. Forecast. Soc. Change 80, 1331–1349. https://doi.org/10.1016/j.techfore.2012.12.006.

Kostoff, R.N., Lau, C.G.Y., 2017. Modified health effects of non-ionizing electromagnetic radiation combined with other agents reported in the biomedical literature. In: Geddes, C. (Ed.), Microwave Effects on DNA and Proteins. Springer, Cham, pp. 97–157 https://doi.org/10.1007/978-3-319-50289-2_4.

Kostoff, R.N., Goumenou, M., Tsatsakis, A., 2018. The role of toxic stimuli combinations in determining safe exposure limits. Toxicol. Rep. 7, 1169–1172. https://doi.org/10.1016/j.toxrep.2018.10.010.

Kumar, P., Nagarajan, A., Uchil, P.D., 2018. Analysis of cell viability by the MTT assay. Cold Spring Harb Protoc 2018, 6. https://doi.org/10.1101/pdb.prot095505.

Lawal, A.O., 2018. Diesel exhaust particles and the induction of macrophage activation and dysfunction. Inflammation 41, 356–363. https://doi.org/10.1007/s10753-017-0682-6.

Leclerc, L., Boudard, D., Pourchez, J., Forest, V., Sabido, O., Bin, V., Palle, S., Grosseau, P., Bernache, D., Cottier, M., 2010. Quantification of microsized fluorescent particles phagocytosis to a better knowledge of toxicity mechanisms. Inhal. Toxicol. 22, 1091–1100. https://doi.org/10.3109/08958378.2010.522781.

Lee, J.H., Moon, S.H., Kim, H.S., Park, E., Ahn, Du., Paik, H.D., 2017. Immune-enhancing activity of phosvitin by stimulating the production of pro-inflammatory mediator. Poult. Sci. 1 (96), 3872–3878. https://doi.org/10.3382/ps/pex205.

Leiro, J.M., Álvarez, E., Arranz, J.A., Cano, E., Orallo, F., 2004. Antioxidant activity and inhibitory effects of hydralazine on inducible NOS/COX-2 gene and protein expression in rat peritoneal macrophages. Int. Immunopharmacol. 4, 163–177. https://doi.org/10.1016/j.intimp.2003.10.004.

Leszczynski, D., Joenvaara, S., Reivinen, J., Kuokka, R., 2002. Non-thermal activation of the hsp27/p38MAPK stress pathway by mobile phone radiation in human endothelial cells: molecular mechanism for cancer-and blood-brain barrier-related effects. Differentiation 70, 120–129. https://doi.org/10.1046/j.1432-0436.2002.700207.x.

Leszczynski, D., Nylund, R., Joenvaara, S., Reivinen, J., 2004. Applicability of discovery science approach to determine biological effects of mobile phone radiation. Proteonomics 4, 426–431. https://doi.org/10.1002/pmic.200300646.

Li, S.P., Junttila, M.R., Han, J., Kahari, V.M., Westermarck, J., 2003. p38 mitogen-activated protein kinase pathway suppresses cell survival by inducing dephosphorylation of mitogen-activated protein/extracellular signal-regulated kinase kinase 1,2. Cancer Res. 63, 3473–3477. https://doi.org/10.1158/0008-5472.CAN-19-3320.

Liu, Q., Hofmann, P.A., 2004. Protein phosphatase 2^a mediated cross-talk between p38 MAPK and ERK in apoptosis of cardiac myocytes. Am. J. Physiol. Heart Circ. Physiol. 286, H2204–H2212.

López-Castejón, G., Brough, D., 2011. Understanding the mechanism of IL-1β secretion. Cytokine Growth Factor Rev. 22, 189–195. https://doi.org/10.1016/j.cytogfr.2011.10.001.

López-Furelos, A., Leiro-Vidal, J.M., Salas-Sánchez, A.A., Ares-Pena, F.J., López-Martín, M.E., 2016. Evidence of cellular stress and caspase-3 resulting from a combined two-frequency signal in the cerebrum and cerebellum of Sprague–Dawley rats. Oncotarget 7, 64674–64689. https://doi.org/10.18632/oncotarget.11753.

López-Furelos, A., Salas-Sánchez, A.A., Ares-Pena, F.J., Leiro-Vidal, J.M., López-Martín, M.E., 2018. Exposure to radiation from single or combined radiofrequencies provokes macrophage dysfunction in the RAW 264.7 cell line. Int. J. Radiat. Biol. 94, 607–618. https://doi.org/10.1080/09553002.2018.1465610.

Lu, Z., Xu, S., 2006. ERK1/2 MAP kinases in cell survival and apoptosis. IUBMB Life 58, 621–631. https://doi.org/10.1080/15216540600957438.

Lu, Z., Xu, S., Joazeiro, C., Cobb, M.H., Hunter, T., 2002. The PHD domain of MEKK1 acts as an E3 ubiquitin ligase and mediates ubiquitination and degradation of ERK1/2. Mol. Cell 9, 945–956. https://doi.org/10.1016/S1097-2765(02)00519-1.

Nel, A., 2005. Atmosphere. Air pollution-related illness: effects of particles. Science 308, 804–806. https://doi.org/10.1126/science.1108752.

Nemoto, Y., Otsuka, T., Niiro, H., Izuhara, K., Yamaoka, K., Nakashima, H., Niho, Y., 1999. Differential effects of interleukin-4 and interleukin-10 on nitric oxide production by murine macrophages. Inflamm. Res. 48, 643–650. https://doi.org/10.1007/s000110050516.

Niranjan, R., Thakur, A.K., 2017. The toxicological mechanisms of environmental soot (black carbon) and carbon black: focus on oxidative stress and inflammatory pathways. Front. Immunol. 30, 763. https://doi.org/10.3389/fimmu.2017.00763.

Osornio-Vargas, A.R., Bonner, J.C., Alfaro-Moreno, E., Martínez, L., García-Cuellar, C., Ponce-de-León Rosales, S., Miranda, J., Rosas, I., 2003. Proinflammatory and cytotoxic effects of Mexico city air pollution particulate matter in vitro are dependent on particle size and composition. Environ. Health Perspect. 111, 1289–1293. https://doi.org/10.1289/ehp.5913.

Pall, M.L., 2018. Wi-Fi is an important threat to human health. Environ. Res. 164, 405–416. https://doi.org/10.1016/j.envres.2018.01.035.

Park, J.S., Carter, S., Reardon, D.B., Schmidt-Ullrich, R., Dent, P., Fisher, P.B., 1999. Roles for basal and stimulated p21 (Cip-1/WAF1/MDA6) expression and mitogen-activated protein kinase signaling in radiation-induced cell cycle checkpoint control incarcinoma cells. Mol. Biol. Cell 10, 4231–4246. https://doi.org/10.1091/mbc.10.12.4231.

Patel, M.M., Chillrud, S.N., Deepti, K.C., Ross, J.M., Kinney, P.L., 2013. Traffic-related air pollutants and exhaled markers of airway inflammation and oxidative stress in New York City adolescents. Environ. Res. 121, 71–78. https://doi.org/10.1016/j.envres.2012.10.012.

Pilla, A.A., 2012. Electromagnetic fields instantaneously modulate nitric oxide signaling in challenged biological systems. Biochem. Bioph. Res. Co. 426, 330–333. https://doi.org/10.1016/j.bbrc.2012.08.078.

Ritz, S.A., 2010. Air pollution as a potential contributor to the 'epidemic' of autoimmune disease. Med. Hypotheses 74, 110–117. https://doi.org/10.1016/j.mehy.2009.07.033.

Rosales, C., Uribe-Querol, E., 2017. Phagocytosis: a fundamental process in immunity. Biomed. Res. Int. 2017, 9042851. https://doi.org/10.1155/2017/9042851.

Rosen, A.D., 2003. Mechanism of action of moderate-intensity static magnetic fields on biological system. Cell Biochem. Biophys. 39, 163–173. https://doi.org/10.1385/CBB:39:2:163.

Ross, C.L., Teli, T., Harrison, B.S., 2016. Electromagnetic field devices and their effects on nociception and peripheral inflammatory pain mechanisms. Altern. Ther. Health Med. 22, 52–64. https://doi.org/10.4258/hir.2016.22.3.156.

Sakamoto, N., Hayashi, S., Gosselink, J., Ishii, H., Ishimatsu, Y., Mukae, H., Hogg, J.C., van Eeden, S.F., 2007. Calcium dependent and independent cytokine synthesis by air pollution particle-exposed human bronchial epithelial cells. Toxicol. Appl. Pharmacol. 225, 134–141. https://doi.org/10.1016/j.taap.2007.07.006.

Salas-Sánchez, A.A., López-Furelos, A., Rodríguez-González, J.A., Ares-Pena, F.J., López-Martín, M.E., 2019. Validation of potential effects on human health of in vivo experimental models studied in rats exposed to sub-thermal radiofrequency. Possible health risks due to the interaction of electromagnetic pollution and environmental particles. IEEE Access 7, 79186–79198. https://doi.org/10.1109/ACCESS.2019.2923581.

Salas-Sánchez, A.A., Rauch, J., López-Martín, M.E., Rodríguez-González, J.A., Franceschetti, G., Ares-Pena, F.J., 2020. Feasibility study on measuring the particulate matter level in the atmosphere by means of Yagi-Uda-Like Antennas. Sensors 20, 3225. https://doi.org/10.3390/s20113225.

Saliev, T., Baiskhanova, D.M., Akhmetova, A., Begimbetova, D.A., Akishev, M., Kulsharova, G., Molkenov, A., Nurgozhin, T., Alekseyeva, T., Mikhalovsky, S., 2019. Impact of electromagnetic fields on in vitro toxicity of silver and graphene nanoparticles. Electromagn Biol Med. 38, 21–31. https://doi.org/10.1080/15368378.2018.1534740.

Schins, R.P.F., Lightbody, J.H., Borm, P.J.A., Shi, T., Donaldson, K., Stone, V., 2004. Inflammatory effects of coarse and fine particulate matter in relation to chemical and biological constituents. Toxicol. Appl. Pharmacol. 195, 1–11. https://doi.org/10.1016/j.taap.2003.10.002.

Schmid Partner Engineering, AG. 2009. Reference manual for the SEMCAD simulation plat-form for electromagnetic compatibility, antenna design and dosimetry. www.semcad.com (accessed on 23 July 2020).

Schwarze, P.E., Øvrevik, J., Hetland, R.B., Becher, R., Cassee, F.R., Låg, M., Løvik, M., Dybing, E., 2007. Importance of size and composition of particles for effects on cells in vitro. Inhal. Toxicol. 19 (Suppl. 1), 17–22. https://doi.org/10.1080/08958370701490445.

Simkó, M., Droste, S., Kriehuber, R., Weiss, D.G., 2001. Stimulation of phagocytosis and free radical production in murine macrophages by 50 Hz electromagnetic fields. Eur. J. Cell Biol. 80, 562–566. https://doi.org/10.1078/0171-9335-00187.

Simko, M., Hartwig, C., Lantow, M., Lupke, M., Mattsson, M.O., Rollwitz, J., 2006. HSP70 expression and free radical release after exposure to non-thermal radio-frequency electromagnetic fields and ultrafine particles inhuman Mono Mac 6 cells. Toxicol. Lett. 161, 73–82. https://doi.org/10.1016/j.toxlet.2005.08.005.

Stuehr, D.J., Marletta, M.A., 1985. Mammalian nitrate biosynthesis: mouse macrophages produce nitrite and nitrate in response to Escherichia coli lipopolysaccharide. PNAS USA 82, 7738–7742. https://doi.org/10.1073/pnas.82.22.7738.

Stuehr, D.J., Marletta, M.A., 1987. Synthesis of nitrite and nitrate in murine macrophage cell lines. Cancer Res. 47, 5590–5594.

Tenuzzo, B., Chionna, A., Panzarini, E., Lanubile, R., Tarantino, P., Di Jeso, B., Dwikat, M., Dini, L., 2006. Biological effects of 6 mT static magnetic fields: a comparative study in different cell types. Bioelectromagnetics 27, 560–577. https://doi.org/10.1002/bem.20252.

Tenuzzo, B., Vergallo, C., Dini, L., 2009. Effect of 6mT static magnetic field on the bcl-2, bax, p53 and hsp70 expression in freshly isolated and in vitro aged human lymphocytes. Tissue Cell. 41, 169–179. https://doi.org/10.1016/j.tice.2008.09.004.

Thomson, E.M., Breznan, D., Karthikeyan, S., MacKinnon-Roy, C., Charland, J.P., Dabek-Zlotorzynska, E., Celo, V., Kumarathasan, P., Brook, J.R., Vincent, R., 2015. Cytotoxic and inflammatory potential of size-fractionated particulate matter collected repeatedly within a small urban area. Part Fibre Toxicol. 12, 24. https://doi.org/10.1186/s12989-015-0099-z.

Vedal, S., Campen, M.J., McDonald, J.D., Larson, T.V., Sampson, P.D., Sheppard, L., Simpson, C.D., Szpiro, A.A., 2013. National particle component toxicity (NPACT) initiative report on cardiovascular effects. Res. Rep. Health Eff. Inst. 178, 5–8. https://doi.org/10.1016/s0273-2300(03)00099-0.

Vince, J.E., De Nardo, D., Gao, W., Vince, A.J., Hall, C., McArthur, K., Simpson, D., Vijayaraj, S., Lindqvist L.M., Bouillet, P., Rizzacasa, M.A., Man, S.M.., Silke, J., Masters, S.L., Lessene, G., Huang, D.C.S., Gray, D.H.D., Kile, B.T., Shao, F., Lawlor, K.E., 2018. The Mitochondrial Apoptotic Effectors BAX/BAK Activate Caspase-3 and -7 to Trigger NLRP3 Inflammasome and Caspase-8 Driven IL-1b Activation. Cell Rep. 25, 2339–2353.e4. doi:https://doi.org/10.1016/j.celrep.2018.10.103

Wallach, D., Varfolomeev, E., Malinin, N.L., Goltsev, Y.V., Kovalenko, A.V., Boldin, M.P., 1999. Tumor necrosis factor receptor and Fas signaling mechanisms. Ann. Rev. Immunol. 17, 331–367. https://doi.org/10.1146/annurev.immunol.17.1.331.

Wang, Q., Schwarz, J.P., Cao, J., Gao, R., Fahey, D.W., Hu, T., Huang, R.-J., Han, Y., Shen, Z., 2014. Black carbon aerosol characterization in a remote area of Qinghai-Tibetan Plateau, Western China. Sci. Total Environ. 479–480, 151–158. https://doi.org/10.1016/j.scitotenv.2014.01.098.

West, M.A., Li, M.H., Seatter, S.C., Bubrick, M.P., 1994. Preexposure to hypoxia or septic stimuli differentially regulates endotoxin release of tumor necrosis factor, interleukin-6, interleukin-1, prostaglandin E2, nitric oxide, and superoxide by macrophages. J. Trauma 37, 82–89. https://doi.org/10.1097/00005373-199407000-00015.

Wójcik-Piotrowicz, K., Kaszuba-Zwoińska, J., Rokita, E., Thor, P., Chrobik, P., Nieckarz, Z., Michalski, J., 2014. Influence of static and alternating magnetic fields on U937 cell viability. Folia Med. Cracov. 54, 21–33.

Wójcik-Piotrowicz, K., Kaszuba-Zwoinska, J., Rokita, E., Nowak, B., Thor, P., 2017. Changes in U937 cell viability induced by stress factors - possible role of Calmodulin. J. Physiol. Pharmacol. 68, 629–636. https://doi.org/10.1039/c7tb02399e.

Wu, C.H., Chen, T.L., Chen, T.G., Ho, W.P., Chiu, W.T., Chen, R.M., 2003. Nitric oxide modulates pro- and anti-inflammatory cytokines in lipopolysaccharide-activated macrophages. J. Trauma 55, 540–545. https://doi.org/10.1097/01.TA.0000033496.62796.3B.

Zagryazhskaya, A.N., Lindner, S.C., Grishina, Z.V., Galkina, S.I., Steinhilber, D., Sudina, G.F., 2010. Nitric oxide mediates distinct effects of various LPS chemotypes on phagocytosis and leukotriene synthesis in human neutrophils. Int. J. Biochem. Cell Biol. 42, 921–931. https://doi.org/10.1016/j.biocel.2010.01.025.